

# Pt- and TiO<sub>2</sub>-doped Nb<sub>2</sub>O<sub>5</sub> Thin Film by Ion-Beam-Enhanced Deposition

Zhu Jianzhong<sup>1</sup> Ren Congxin<sup>2</sup> Mu Haichuan<sup>2</sup>

1 State Key Laboratories of Transducer Technology,

2 Ion Beam Laboratory

Shanghai Institute of Metallurgy, Chinese Academy of Sciences

Shanghai 200050, China

## ABSTRACT

This paper describes the preparation of Pt- and TiO<sub>2</sub>-doped Nb<sub>2</sub>O<sub>5</sub> thin film by Ion-Beam-Enhanced Deposition. Platinum and titanium doping, and Nb<sub>2</sub>O<sub>5</sub> deposition were carried out in situ. The dependence of oxygen sensing properties on the amounts of Pt and Ti dopant in the Nb<sub>2</sub>O<sub>5</sub> film was investigated. There were the highest sensitivity, the lowest temperature coefficient and the shortest response time at doping of 5 mol % TiO<sub>2</sub> and 0.3 mol % Pt

## 1. INTRODUCTION

Oxygen sensors that can operate at elevated temperatures have found wide use in monitoring and control of combustion processes, for example, control of the air-to-fuel mixture of an internal combustion engine. In the most widespread application, the oxygen sensors are used to feedback control the air-to-fuel ratio, A/F, of an engine at the stoichiometric value, (A/F)<sub>stoich</sub>, by detecting the large change in the thermodynamic equilibrium oxygen partial pressure of the exhaust gas that occurs at this A/F value. To date, two different types of these so-called stoichiometric exhaust gas oxygen sensors have been developed. One is an electrochemical oxygen concentration cell made from yttria or calcia-stabilized zirconia (ZrO<sub>2</sub>). The other is a MOS (metal Oxide semiconductor)-based resistive-type device which utilizes the fact that the resistivity of MOS depends on the oxygen partial pressure in the ambient. Among MOS materials, TiO<sub>2</sub> has been under the most investigations [1-3]. Kondo et al [4] have reported that Nb<sub>2</sub>O<sub>5</sub> exhibits the better sensing properties than TiO<sub>2</sub> as an A/F sensing material. Michitaka Chtaki et al [5] also reported that TiO<sub>2</sub>-doped Nb<sub>2</sub>O<sub>5</sub> ball mill exhibits the maximum sensitivity and the smaller temperature dependence on the electrical conductivity at the low doping level of Ti. This paper describes the preparation and characterization of Pt- and TiO<sub>2</sub>-doped Nb<sub>2</sub>O<sub>5</sub> Thin Film by IBED ( Ion-Beam-Enhanced Deposition ). The better performances for oxygen sensing were obtained.

## 2. EXPERIMENTAL

Using the IBED technique and microelectron planar technology, automotive A/F sensors were produced on Al<sub>2</sub>O<sub>3</sub> substrates consisting of an oxygen-sensitive Pt- and TiO<sub>2</sub>-doped Nb<sub>2</sub>O<sub>5</sub> element, a platinum temperature sensor and a Pt heater. (see Fig. 1). The Pt thin film with a thickness of 1 μm was deposited by IBED, and was patterned using a conventional lift-off photolithographic process.

The Pt- and Ti-doped Nb<sub>2</sub>O<sub>5</sub> thin film was deposited on a cooled Al<sub>2</sub>O<sub>3</sub> substrate by IBED using a single ion source with Ar ion from a combined target of Pt, Ti and Nb<sub>2</sub>O<sub>5</sub>( purity concentration 5×10<sup>-3</sup> % w/w). The amount of Pt and Ti dopant in Nb<sub>2</sub>O<sub>5</sub> could be changed by changing area ratio of Pt and Ti to Nb<sub>2</sub>O<sub>5</sub> target (see Fig. 2). The doping dose of Pt and Ti in Nb<sub>2</sub>O<sub>5</sub> could also be finely adjusted by varying IBED parameters such as ion beam energy, ion beam current density and incident angle. The patterns of the Nb<sub>2</sub>O<sub>5</sub> thin film were again delineated using the lift-off technique.

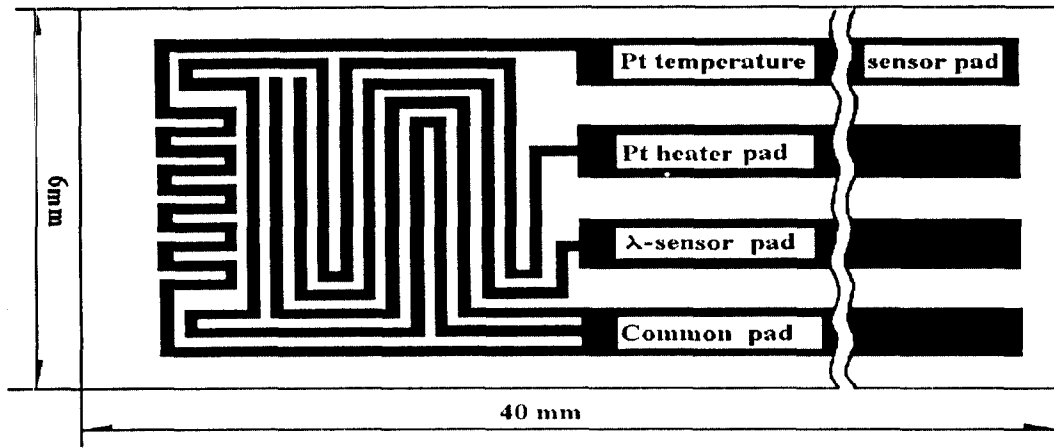


Fig 1. The structure of the  $\lambda$ -sensors

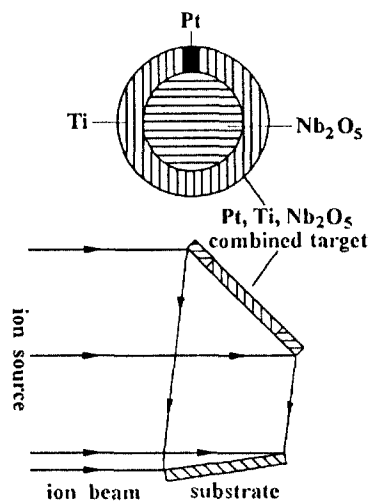


Fig 2. The principle of doping and simultaneous deposition in the IBED system

During deposition, the total pressure in the operation chamber of the sputtering system was approximately  $1.6 \times 10^{-2}$  Pa using 66.7% Ar and 33.3%  $O_2$ . The average sputtering power was approximately  $2W/cm^2$ , which resulted in a deposition rate of 24nm/min. The films with a thickness between 0.5 and  $1.5\mu m$  were then tempered in air for 2h at  $1000^\circ C$  to obtain a structure, that was stable under high temperatures. The films were investigated by electrical measurements, X-ray diffraction (XRD), X-ray photoelectron spectroscopy (XPS). Analysis of the amount of  $TiO_2$  dopant was carried out using inductively coupled plasma atomic emission spectrometry (ICP-AES). The dependence of the electrical resistance of the film on temperature was measured using a quartz vessel in a tube furnace either in nitrogen or oxygen. The R-T characteristic of the specimen was measured in the exhaust gas of an oxygen-propane combustion in the temperature range of  $550$  to  $750^\circ C$ . Propane, oxygen and nitrogen were mixed in appropriate ratios to obtain the desired  $\lambda$  value, then the gas mixture was burned at  $450^\circ C$  over a combustive catalytic case. The exhaust

gas was introduced into the quartz vessel in which an yttria-stabilized zirconia (YSZ) oxygen sensor was installed to monitor the equilibrus partial pressure of oxygen. The resistance of the specimen was measured using a 8840A MULTIMETER. Figure 3 shows the schematic diagram of the measurement system of the sensors.

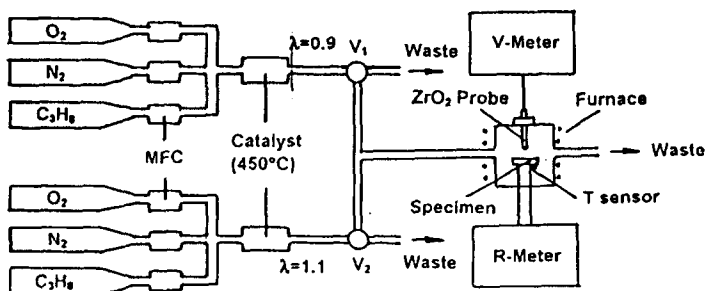


Fig 3. Schematic diagram of the measurement system of the sensors

### 3. Results and discussion

#### 3.1 Spectra of XRD for the films

The results examined by XRD indicated that the  $\text{TiO}_2\text{-Nb}_2\text{O}_5$  films with different ratio exhibit amorphous state. Figure 4 shows the spectra of XRD for the films after annealing at  $1000^\circ\text{C}$  in air for 2h. Besides the pure  $\text{TiO}_2$  film is rutile, the  $\text{Nb}_2\text{O}_5$  films with various amount of  $\text{TiO}_2$  dopant belong to monoclinic system while not to found any  $\text{TiO}_2$  crystal phases until the amount of  $\text{TiO}_2$  dopant up to 34mol %. However, It is confirmed by the spectrum of XPS that Ti in  $\text{Nb}_2\text{O}_5$  films appear as  $\text{TiO}_2$  bond even through annealing at the range of  $900\text{-}1100^\circ\text{C}$  ( Figure 5).

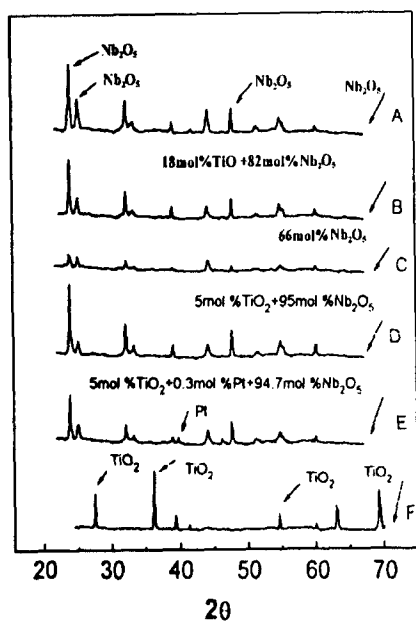


Fig. 4 Spectra of XRD for the films with different component.

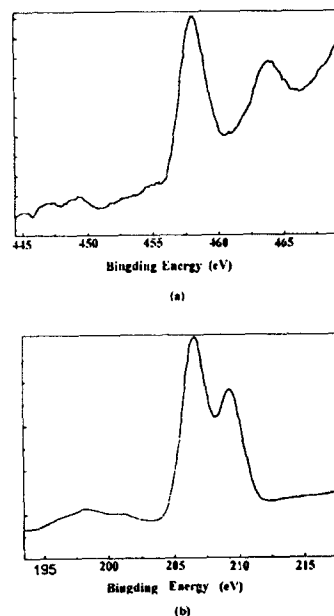


Fig. 5 Spectra of XPS for  $\text{TiO}_2$  (a) and  $\text{Nb}_2\text{O}_5$  (b).

### 3.2 Characteristic factor and activation energy

It is common knowledge that the electrical resistance of metal oxide semiconductor film depends on  $pO_2$  according to the following equation:

$$R = R_0 \exp(E/KT) (P_{O_2})^{1/m}, \quad (1)$$

where  $m$  is a characteristic factor as a measure of the sensitivity to oxygen.  $E$  the activation energy,  $k$  the Boltzman constant.  $T$  the substrate temperature and  $pO_2$  the partial oxygen pressure.

The measured data of the resistance of  $TiO_2$ -doped  $Nb_2O_5$  thin film [ $TiO_2/(TiO_2+Nb_2O_5)=75\text{mol}\%$ ] and the calculated  $m$  values are listed in Table 1.

Table 1 Dependence of the resistance of the sensor on the partial pressure of oxygen at 700°C and the calculated  $m$  values.

Atmosphere	$pO_2$ (KPa)	$R$ (K $\Omega$ )	$m$	$\bar{m}$
$O_2$	100	1050	4.896	
$N_2$	0.01	160	4.896	
$O_2$	100	1010	4.880	4.9
$N_2$	0.01	153	4.880	
$O_2$	100	963	4.918	
$N_2$	0.01	148	4.918	

The characteristic factor  $m$ , the activation energy  $E$  and the constant  $R_0$  of the films for various mol % of  $TiO_2$  to  $Nb_2O_5$  are listed in Table 2. The results shown in Table 2 indicate that the characteristic factor  $m$  decreased, i.e., the sensitivity to oxygen increased and the activation energy  $E$  decreased, so that the effect of temperature on the resistance of the film decreased as the ratio of  $TiO_2$  to  $Nb_2O_5$  decreased. Thus we chose 5 mol %  $TiO_2$  as the film composition for the remaining experiments. The dependence of the characteristic factor  $m$  on the ratio of  $TiO_2$  to  $Nb_2O_5$  is similar to that found by Ohtak et al [5].

Table 2  $m$ ,  $E$  and  $R_0$  of the film depends on the ratio of  $TiO_2$  to  $Nb_2O_5$ .

$TiO_2/(TiO_2+Nb_2O_5)$ (mol%)	$m$	$E$ (eV)	$R_0$ ( $\Omega$ )
75	4.9	0.74	0.24
25	4.9	0.20	4030
5	4.3	0.10	4467

### 3.3 Resistance- $\lambda$ Characteristic curves

The resistance- $\lambda$  characteristic curves at different temperatures are shown in Fig. 6. The jump in the curves at the stoichiometric point is greater than 3 orders of magnitude. There is a greater effect of temperature on the resistance of the sensor in the lean-burning region and little effect in the rich-burning region in the temperature range of 600 to 750 °C. Hence, the resistance jump of the sensor at low temperatures is larger than at high temperatures.

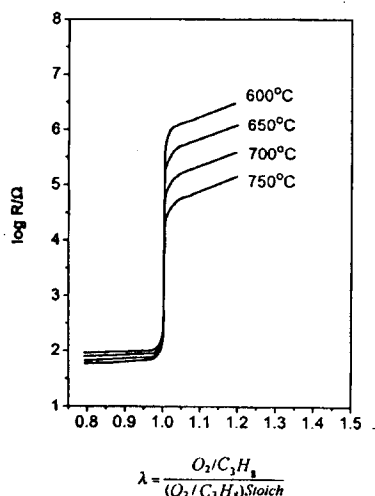


Fig 6 Resistance- $\lambda$  characteristic curve of the  $\lambda$ -sensor at different temperatures.

### 3.4 Response time

The response time of the sensor depends not only on the temperature of the substrate and the thickness of the sensitive film (diffusion within a solid), but also on various other factors, including gas diffusion, absorption, reaction and porous diffusion as well as on the gas species of environment and the catalyst in the film. There were no significant differences for response time between the sensor without the catalyst Pt and that with Pt when the atmosphere changed between nitrogen and oxygen and between propane and oxygen. It took 3.5 min to establish a stable response when the atmosphere changed from nitrogen to oxygen. However, the response time of the sensor is shorter than 0.1 min when the atmosphere changed from propane to oxygen. When the atmosphere changed from  $\lambda=1.1$  to 0.9, the response time of the sensor with 0.03mol% of Pt was shorter than that without Pt. Compared with  $ZrO_2$  oxygen sensor (LSH 23 Bosch, Germany), the response time of the  $Nb_2O_5$  film sensor (10 ms) is shorter than that of the  $ZrO_2$  sensor (20 ms) when the atmosphere changes from  $\lambda=0.9$  to 1.1, which is contrary to that when  $\lambda=1.1$  to 0.9 (100ms and 20 ms, respectively) (Fig. 7).

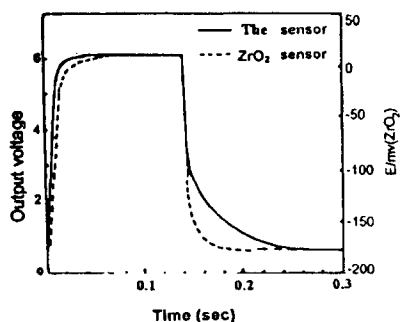


Fig.7. Comparison between the response time for the sensor and that for  $ZrO_2$  oxygen sensor at 600°C when  $\lambda$  changes from 0.9 to 1.1 and vice versa.

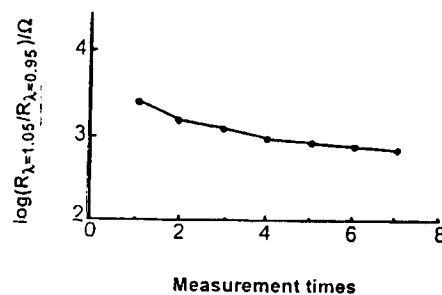


Fig.8. The resistance jump at the stoichiometric point in the characteristic curves which changes with the measurement time.

### 3.5 Stability

Equation(1) shows that the lower the activation energy, the lower the TCR(temperature coefficient of resistance) for oxygen-sensitive film. That is, the higher the thermostability for the oxygen-sensitive device. Figure 8 shows the stability of the  $\lambda$ -sensor. Initially the  $\lambda$ -sensor presented a high sensitivity which then decreased slightly as the time for measuring increased, and it became stable after seven measurements were taken. Therefore, to carry out the aging process, the stable response characteristic of the sensors must be obtained.

### 4. Conclusion

A new automotive air/fuel sensor based on Pt- and TiO<sub>2</sub>-doped Nb<sub>2</sub>O<sub>5</sub> thin film was developed using the IBED technique and planar microsystem technology. The sensor performed well, exhibiting such factors as high sensitivity and good stability, as well as the possibility of cost-effective production. However, further studies are needed to produce a  $\lambda$ -sensor with optimum performance that can be applied to automotives. For example, it is necessary to place a protective layer on the surface of oxygen-sensitive films to reduce the adverse effects, specifically those due to the poison action of lead, sulfur and phosphorus.

### Acknowledgement

The authors gratefully acknowledge financial support from Ford and NSFC, Shanghai R & D Fund, State Key Laboratory of Transducer Technology and Ion Beam Laboratory , Chinese Academy of Sciences.

### References

- 1 T.Y. Tien, H.L.stadler, E.F. Gibbons and P.J. Zacmanidis, *Ceram. Bull.*, 54(1975)280.
- 2 E.M. Logothetis and W.J. Kaiser, *Sensors and Actuators*,4(1980)333.
- 3 E.M. Logothetis: automotive oxygen sensor, *Chemical Sensor Technology*, Vol.3 ed. N.Yamazoe, (Kodanasha, Tokyo/Elsevier, Amsterdam, 1991), 89.
- 4 H. Kondo, H. Takahashi, T. Takeuchi and I. Igarashi, *Proc. 3rd Sensor Symp.*, Japan, 1983, p.185.
- 5 Michitaka Ohtak, Jun Peng, Koichi Eguchi and Hiromichi Arai: *Sensors and Actuators B13-14* (1993)495.
- 6 H.J.Beie and A.Gnorich:*Sensors and Actuators B4* (1991) 393.